A Structural Motif of Acetylcholinesterase That Promotes Amyloid β-Peptide Fibril Formation†

Giancarlo V. De Ferrari,‡ Mauricio A. Canales,§ Irina Shin,|| Lev M. Weiner,|| Israel Silman,⊥,# and Nibaldo C. Inestrosa*,‡,▼

Center for Cell Regulation and Pathology, Department of Cell and Molecular Biology, Faculty of Biological Sciences, P. Catholic University of Chile and Millenium Institute for Fundamental and Applied Biology, Santiago, Chile, Department of Molecular Biology, University of Concepción, Concepción, Chile, and Departments of Chemical Services and Neurobiology, The Weizmann Institute of Science, Rehovot, Israel

Received January 22, 2001; Revised Manuscript Received May 31, 2001

ABSTRACT: Acetylcholinesterase (AChE) has been found to be associated with the core of senile plaques. We have shown that AChE interacts with the amyloid β-peptide (Aβ) and promotes amyloid fibril formation by a hydrophobic environment close to the peripheral anionic binding site (PAS) of the enzyme. Here we present evidence for the structural motif of AChE involved in this interaction. First, we modeled the docking of Aβ onto the structure of *Torpedo californica* AChE, and identified four potential sites for AChE−Aβ complex formation. One of these, *Site I*, spans a major hydrophobic sequence exposed on the surface of AChE, which had been previously shown to interact with liposomes [Shin et al. (1996) *Protein Sci. 5*, 42−51]. Second, we examined several AChE-derived peptides and found that a synthetic 35-residue peptide corresponding to the above hydrophobic sequence was able to promote amyloid formation. We also studied the ability to promote amyloid formation of two synthetic 24-residue peptides derived from the sequence of a Ω-loop, which has been suggested as an AChE−Aβ interacting motif. Kinetic analyses indicate that only the 35-residue hydrophobic peptide mimics the effect of intact AChE on amyloid formation. Moreover, RP-HPLC analysis revealed that the 35-residue peptide was incorporated into the growing Aβ-fibrils. Finally, fluorescence binding studies showed that this peptide binds Aβ with a K_d = 184 μM, independent of salt concentration, indicating that the interaction is primarily hydrophobic. Our results indicate that the homologous human AChE motif is capable of accelerating Aβ fibrillogenesis.

The amyloidoses are a group of protein misfolding disorders characterized by accumulation of insoluble fibrillar protein complexes in the extracellular space (*1*). To date, several proteins and polypeptides have been identified in amyloid deposits, including the islet-associated polypeptide in type II diabetes, the prion protein in the transmissible spongiform encephalopathies, and the 39−43-residue amyloid β-peptide (Aβ)[1] in Alzheimer's disease (AD) (*2*). With respect to AD, diverse lines of evidence have suggested that aggregation and deposition of Aβ are major events in the appearance and development of the disease (*3*). It is presently thought that Aβ is generated intracellularly by proteolytic processing of the amyloid precursor protein (APP) (*4*), and that in order to acquire its pathogenic condition, it requires an active change in its molecular structure (*5*). Such a transition, from a nonpathogenic soluble conformation to one capable of assembly into amyloid fibrils, has been proposed to be a nucleation-dependent process that can be modulated by physicochemical factors and enhanced by the presence of "companion" or "chaperone" molecules (*6*).

Acetylcholinesterase (AChE; EC 3.1.1.7) plays a key role in cholinergic neurotransmission (*7*, *8*), and may also fulfill noncholinergic roles (*9*). It has been observed that in AD brains cortical AChE activity is associated predominantly with the amyloid core of mature senile plaques, pre-amyloid diffuse deposits, and cerebral blood vessels (*10*). Previous studies have indicated that AChE binds to Aβ and induces Aβ fibril formation (*11*), forming a macromolecular complex

† This work was supported by FONDECYT Grant 2970073 (to G.V.D.F.), by FONDAP Grant 1389001 and MIFAB Grant 2398969 (to N.C.I.), and by an Israel Science Foundation grant (to L.M.W. and I.S.).

* To whom correspondence should be addressed at the Centro de Regulación Celular y Patología, Depto. de Biología Celular y Molecular, Fac. Ciencias Biológicas, P. Universidad Católica de Chile, Alameda 340, P.O. Box 114-D, Santiago, Chile. Tel: 56-2-6862720, FAX: 56-2-6862959, E-mail: ninestr@genes.bio.puc.cl.

‡ Department of Cell and Molecular Biology, P. Catholic University of Chile and Millenium Institute for Fundamental and Applied Biology.

§ Department of Molecular Biology, University of Concepción.

|| Department of Chemical Services, The Weizmann Institute of Science.

⊥ Department of Neurobiology, The Weizmann Institute of Science.

I.S. is a Bernstein−Mason Professor of Neurochemistry.

▼ N.C.I. is recipient of a Presidential Chair in Science from the Chilean Government (1999−2001) and a John Simon Guggenheim Foundation Fellowship.

[1] Abbreviations: AChE, acetylcholinesterase; AD, Alzheimer's disease; Aβ, amyloid β-peptide; PAS, peripheral anionic site; RP-HPLC, reversed-phase high-performance liquid chromatography.

10.1021/bi0101392 CCC: $20.00
Published on Web 08/08/2001

with the growing fibrils (*12*). These studies suggested that a specific motif, located close to the rim of the active-site gorge of the enzyme, termed the "peripheral" anionic site (PAS) (*13*), might be involved in accelerating fibril formation, since both PAS inhibitors (*11*) and a monoclonal antibody directed toward the PAS (*14*) blocked the amyloidogenic effect of AChE. In a recent study on the crystal structure of mouse AChE, Bourne et al. (*15*) suggested that human AChE may interact with Aβ through a short Ω-loop located in the vicinity of the PAS. We report in the following, molecular modeling studies and physicochemical analyses that identify a different structural motif in AChE responsible for its interaction with Aβ. From a pharmacological perspective, this study is aimed at understanding the mechanism by which the complex AChE−Aβ is formed, and thus helping in the development of new drugs to prevent or delay the selective death of the cholinergic circuitry observed in AD brains.

EXPERIMENTAL PROCEDURES

Synthetic Peptides. Aβ corresponding to residues of the human wild-type Aβ_{1-40} sequence, and a variant Aβ_{1-40} peptide containing a valine-to-alanine substitution (Val18→Ala) (*5*) were obtained from Chiron Corp. Inc., Emeryville, CA. A hydrophobic polypeptide ($H_{274-308}$), corresponding to residues Leu274−Met308 of *Torpedo* AChE (Figure 1), and a polypeptide corresponding to residues Ala252−Thr275 of mouse AChE ($\Omega_{252-275}$), cycled by a disulfide bridge between its Cys257 and Cys272 residues, as well as its corresponding linear homologue were all purchased from U. S. Peptides Inc., Fullerton, CA. All peptides were further purified by reverse-phase high-performance liquid chromatography (RP-HPLC), and stock solutions were prepared as previously described (*12*).

Docking of Aβ onto Torpedo AChE. Two Aβ models, built by homology modeling from a fragment of the enzyme triosephosphate isomerase (*16*), were used for docking. The first one was minimized locally using AMBER (*17*), and the second was obtained after 90 ps of molecular dynamics simulation. Docking of Aβ was done using GRAMM (*18*), which is the best protein−protein docking procedure classified on CASP2 (*19*). All modeled structures were positioned arbitrarily, adjacent to the high-resolution structure of *Torpedo californica* AChE (PDB code: 2ACE), and according to the requirements of GRAMM, they contained coordinates for hydrogen atoms. The parameters used by GRAMM were as follows: nmode = generic, grid-step = 6.8 and 1.7, potential range type = grid-step, representation all, angle for rotations = 20°. Such parameters allow calculation of electrostatic interactions between proteins at high resolution (*18*). Those positions that presented only different translational coordinates were selected from the output list of GRAMM and then sorted by their interaction energy (not shown).

Purification of AChE from Bovine Brain and from Torpedo. The tetrameric G_4 form of AChE from bovine caudate nucleus was purified using acridine-affinity chromatography as described (*20*). The dimeric G_2 form of AChE from *Torpedo* electric organ was purified by affinity chromatography after solubilization with phosphatidylinositol-specific phospholipase C or by extraction at low ionic strength in the presence of Triton X-100, as described (*21*, *22*).

Aβ Aggregation Assay. Aggregation was monitored as described by Evans et al. (*23*). In brief, stock solutions were prepared by dissolving lyophilized Aβ aliquots in dimethyl sulfoxide (DMSO) at 12.5 mg/mL (6.4 mM). Aliquots of Aβ peptide stock (128 nmol in $\cong$20 μL of DMSO) were added to 700 μL of 10 mM Tris-HCl, pH 7.4, in water. When aggregation assays were performed in the presence of mammalian or *Torpedo* AChE or of AChE-derived peptides, the Aβ peptide stock solution was added to the same aqueous Tris buffer containing AChE, or the peptides, at the concentrations stated in the text or in the figures. The solutions were stirred continuously (210 rpm) at room temperature, and aggregation was followed by measuring turbidity at 405 nm.

Quantitation of Amyloid Formation. To quantify amyloid formation, the thioflavine T (Th-T) fluorescence method (*24*) and the Congo-Red (CR) assay (*25*) were both used as described previously (*11*, *12*).

Electron Microscopy of Amyloid Fibrils. Amyloid fibrils formed either in the absence or in the presence of *Torpedo* AChE or the hydrophobic AChE-derived peptide were collected by centrifugation for 30 min at 14 000 rpm in an Eppendorf microcentrifuge. The pellet was washed 3 times with 1 mL of 10 mM Tris-HCl, pH 7.4, to wash out soluble material. The fibrils were placed on Formvar-carbon coated 300-mesh nickel grids, negatively stained with 2% uranyl acetate (Ladd) for 60 s, and visualized on a Siemens 1 Å electron microscope at 60 kV (*11*, *12*).

Reverse-Phase HPLC Analysis. Incorporation of the AChE-derived peptides into amyloid fibrils was analyzed by reversed-phase HPLC (RP-HPLC) on a Delta Pak C-18 column (3.9 × 150 mm, Waters), using a Waters model 600-E HPLC apparatus. As previously stated, the amyloid fibrils formed in the turbidity assays were collected by centrifugation (as described above), and the pellet was washed 3 times with 1 mL of Tris-HCl (pH 7.4) in order to eliminate soluble material. The pellet was resuspended in a final volume of 100 μL and loaded onto the reverse-phase column preequilibrated with 0.1% (v/v) trifluoroacetic acid in water. The column was eluted with a linear gradient of 0−80% (v/v) acetonitrile in 0.1% (v/v) trifluoroacetic acid/water over 50 min, and the effluent was monitored at 214 nm as described previously (*26*).

Binding Studies. Interaction of the *Torpedo* $H_{274-308}$ peptide with Aβ was monitored by fluorescence spectroscopy using a Shimadzu RF-540 model spectrofluorometer. Briefly, 7.3 μg of $H_{274-308}$ (in 3 μL of DMSO) was dissolved in 200 μL of 10 mM Tris-HCl, pH 7.4, and the fluorescence emission spectrum was recorded immediately between 300 and 400 nm, with excitation at 295 nm, and slits set at 5 nm bandwidth. Increasing concentrations of Aβ (17−170 μM in DMSO) were added to the $H_{274-308}$ solution, and a fluorescence spectrum was recorded at each concentration after 15 min of co-incubation. Binding was evaluated from both the change in emission intensity and the shift in emission maximum.

Software. Docking calculation results were analyzed on an INDY machine using Homology and Insight II (Biosym/MSI). Graphic visualizations were performed using the program WebLab ViewerLite 3.01 (Molecular Simulations,

FIGURE 1: CLUSTAL-W multiple sequence alignment of AChE sequences from different species. Sequences corresponding to the synthetic AChE peptides used in this study. Red: 24-residue peptide from mouse AChE ($\Omega_{252-275}$; mammalian numbering); blue: 35-residue peptide from *Torpedo* AChE ($H_{274-308}$; *Torpedo* numbering). The PAS residues Tyr70 and Trp279 corresponding to the *Torpedo* sequence (Tyr72 and Trp286, respectively, according to mammalian numbering) are labeled with a red asterisk. Depicted as boxes are Cys residues that form the disulfide bridge of the Ω-loop. Mammalian sequences correspond to subunits of type T and the *Torpedo* sequence to subunit of type H. Note the 4-residue gap in the sequence of *Torpedo* AChE within the Ω-loop.

Inc.). Binding data were analyzed with the aid of curve-fitting software (Origin Microcal, 4.1, http://www.microcal.com). Multiple Sequence Alignment was done with CLUSTAL-W (http://www2.ebi.ac.uk/clustalw/).

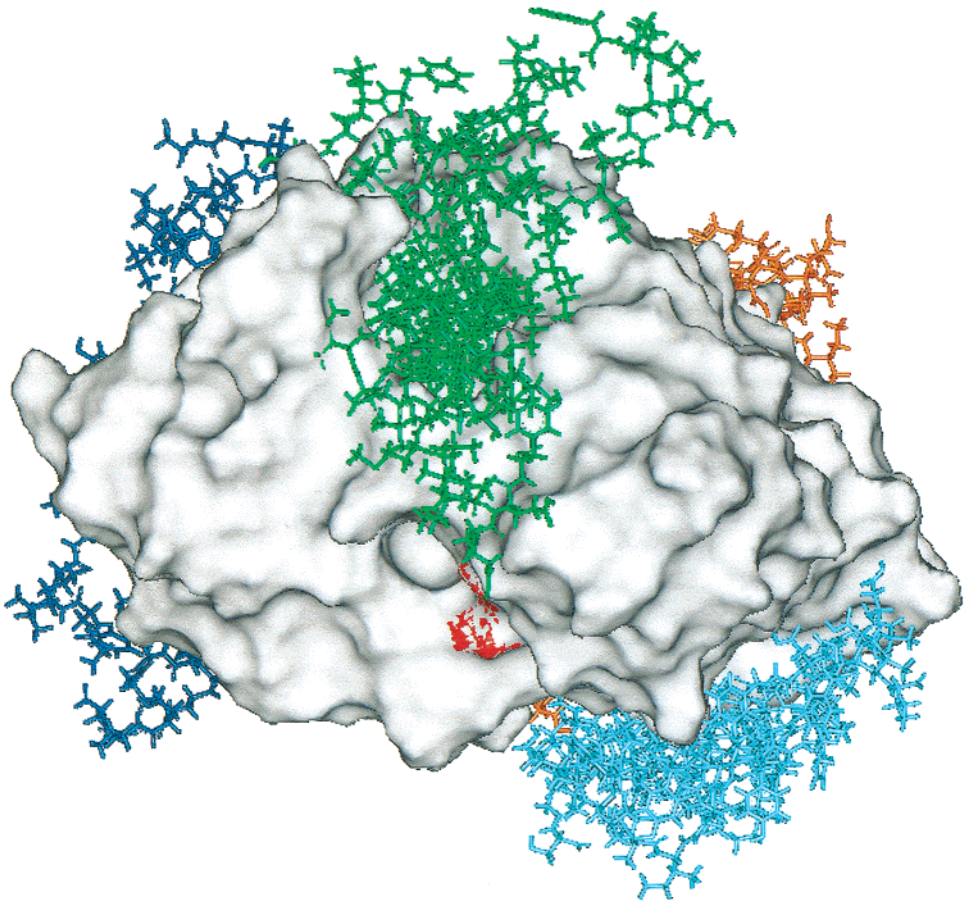

FIGURE 2: Docking simulation of Aβ on *Torpedo* AChE. Overall view of the surface of *Torpedo* AChE and the putative docking sites for Aβ. *Site I*, green; *Site II*, blue; *Site III*, turquoise; *Site IV*, orange. Looking straight into the active-site gorge, the representative surface for the PAS residues Tyr70 and Trp279 is displayed in red. Conformations of all proteins were not modified during docking, as described by Vakser (*18*). The localization of model peptides on AChE sites suggests that the principal interactions are along the main axis of the peptide.

RESULTS

Docking of Aβ onto Torpedo AChE. We recently proposed a model for the complete Aβ structure (Aβ_{1-40}) by molecular modeling based on extensive homology to an α/β segment of the enzyme triosephosphate isomerase (*16*). Accordingly, we used our Aβ model as a template to identify motifs in the 3D structure of *Torpedo* AChE which might interact with Aβ. We chose to work with *Torpedo* rather than with mouse AChE since, although their 3D structures are almost identical, the *Torpedo* structure has been determined to substantially higher resolution. Four putative binding sites for Aβ were identified on the surface of *Torpedo* AChE using our modeled Aβ structure: *Site I* includes residues Pro232, Val236, Val281−Ser286, Arg289, Ser307, Asn310, and Pro361−His362 of the enzyme (Figure 2, green). *Site II* includes Lys325, Glu344, Tyr375−Thr376, His 425, Glu514, and Val518−Met520 (Figure 2, blue). *Site III* includes Pro21, Trp58−Asn60, Thr62, and Glu89−Met90 (Figure 2, turquoise). *Site IV* includes Pro106−Ser108, Thr138−Glu140, Lys454, Lys478, and Ser487 (Figure 2, orange). Interestingly, *Site I* overlaps with a sequence in *Torpedo* AChE which interacts with liposomes and contains the PAS residue, Trp279 (*27*).

Torpedo AChE Promotes Aβ Aggregation into Amyloid Fibrils, and a 35 aa Hydrophobic Peptide Derived from Its Sequence Displays Similar Activity. We demonstrated earlier that AChE extracted and purified from various species was able to induce formation of amyloid fibrils (*11*). To validate our docking model and to extend our previous results, we examined whether *Torpedo* AChE also induced Aβ polymerization into amyloid fibrils. The dimeric (G_2) form of *Torpedo* AChE, whether purified either by solubilization with PI-PLC or by extraction at low ionic strength in the presence of Triton X-100 (*21*, *22*), was indeed able to induce amyloid formation (Figure 3A), thus permitting *Torpedo* AChE to serve as a docking paradigm.

Aβ has a marked tendency to interact with hydrophobic environments (*28*, *29*), and we have presented evidence that hydrophobic interactions may play a role in stabilization of the AChE−Aβ complex (*12*). Shin et al. (*27*) have shown that a dimeric form of *Torpedo* AChE can interact with small liposomes of dimyristoylphosphatidylcholine (DMPC) through a 5-kDa hydrophobic polypeptide sequence, which is exposed when the protein partially unfolds either upon mild denaturation or as a result of chemical modification. Therefore, as a first attempt to identify the AChE motif involved in the interaction with Aβ, we examined the ability to stimulate amyloid fibril formation of a synthetic 35-residue peptide corresponding to residues Leu274−Met308 ($H_{274-308}$) of TcAChE (Figure 1), which roughly corresponds to *Site I*, and contains some of the residues that contact Aβ in our docking model. Figure 3B shows that this peptide was indeed

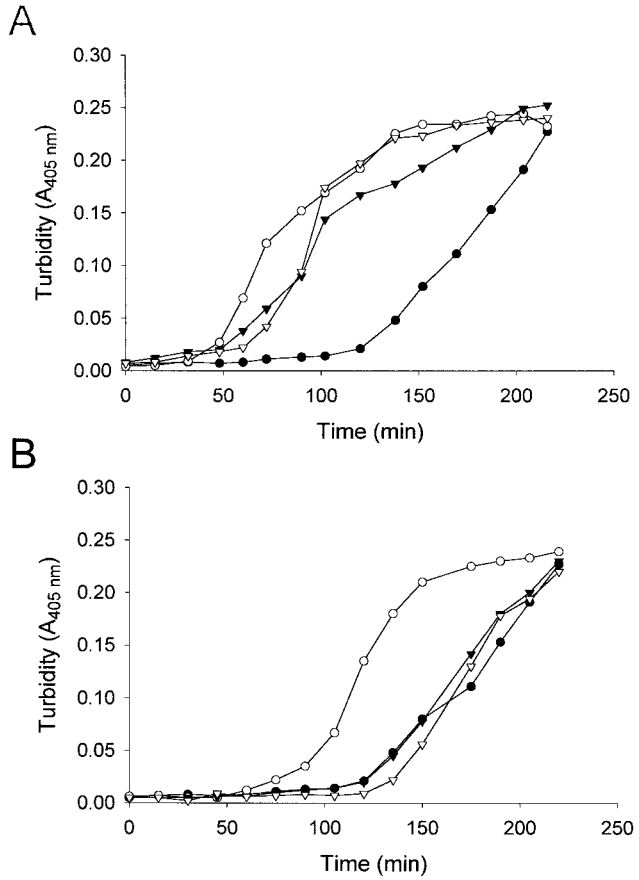

FIGURE 3: *Torpedo* AChE and its derived $H_{274-308}$ peptide induce Aβ fibril formation. (A) 300 μg of Aβ was incubated either alone (●) or in the presence of 25 μg of *Torpedo* AChE (G_2) solubilized with PI-PLC (▽) or at low ionic strength in the presence of detergent (▼), and with bovine brain AChE (G_4; ○), at a molar ratio of Aβ:AChE monomer = 200:1. (B) 300 μg of Aβ was incubated either alone (●) or in the presence of 3 μg of the *Torpedo* $H_{274-308}$ peptide (○) or the mouse-derived $\Omega_{252-275}$ peptides (▽, Cys-Cys disulfide linked; ▼, linear), at a molar ratio of Aβ:peptide = 100:1 in aqueous buffer (725 μL of 10 mM Tris-HCl, pH 7.4).

Table 1: Analysis of Kinetic Parameters of Amyloid Fibril Formation

peptides	lag time[a] (min, ±SE)	relative exponential growth rate[b] (Abs/min)
Aβ_{1-40}	110.7 ± 10.3	1.97
Aβ_{1-40} + AChE	45.2 ± 8.8	2.65
Aβ_{1-40} + $H_{274-308}$[c]	71.4 ± 5.3	2.71
Aβ_{1-40} + cycled $\Omega_{252-275}$[d]	115.5 ± 6.7	1.83
Aβ_{1-40} + linear $\Omega_{252-275}$[d]	108.6 ± 4.6	1.88

[a] Determined from the beginning of a turbidimetric assay to the intersection with the slope of the exponential growth phase. [b] Linear regression analysis of the exponential growth phase. [c] Synthetic fragment derived from TcAChE sequence. [d] Synthetic fragment derived from mouse AChE sequence.

able to mimic the effect of AChE on Aβ fibril formation (see also Table 1). At a molar ratio of 1:100, the $H_{274-308}$ peptide decreased the lag phase for Aβ aggregation similarly to *Torpedo* AChE, although to a lesser degree. In contrast, both a 24-residue polypeptide corresponding to residues Ala252−Thr275 of mouse AChE ($\Omega_{252-275}$), cycled by a disulfide bridge between its Cys257 and Cys272 residues (Figure 1), which had been proposed as a putative motif for AChE−Aβ interaction (*15*), and also its corresponding linear homologue (same sequence but not disulfide-linked) had no effect on fibril formation (Figure 3B). None of the synthetic peptides incubated alone formed any visible aggregates (same concentration of Aβ, 100 μM, not shown). Finally, the aggregates formed by Aβ, whether alone or in the presence of either *Torpedo* AChE or the *Torpedo* $H_{274-308}$ peptide, were shown to be amyloid on the basis of both the Th-T and the CR assays. Aliquots taken at the final time point from each sample showed no differences in the affinity for either Th-T (Figure 4A) or CR (Figure 4B), confirming that the aggregates were indeed amyloid fibrils. Moreover, examination of the samples by electron microscopy revealed no major differences in the morphology of the amyloid fibrils induced by *Torpedo* AChE or by the $H_{274-308}$ peptide (Figure 4C).

The TcAChE Fragment Is Incorporated into the Growing Aβ Fibrils in a Concentration-Dependent Manner. During the process of amyloid formation, AChE is incorporated into growing Aβ fibrils (*12*). We therefore examined, at the end of an aggregation assay with stirring, whether the AChE-derived peptides were similarly incorporated into Aβ fibrils. Figure 5 shows RP-HPLC elution profiles of samples loaded onto a C-18 column and eluted with a linear gradient of 0−80% acetonitrile. Panel A shows the elution profiles of increasing concentrations of the *Torpedo* $H_{274-308}$ peptide alone (retention time ca. 24 min). Panel B shows the profiles of amyloid fibrils formed by the Aβ peptide grown alone (left, retention time ca. 18 min) or by coincubating the Aβ peptide with the *Torpedo* $H_{274-308}$ peptide. As can be seen, both peptides can be detected as single peaks in the same run; thus binding of the *Torpedo* peptide to Aβ is clearly demonstrated. Finally, the mouse-derived $\Omega_{252-275}$ peptides were not incorporated into amyloid fibrils (not shown). We reported earlier that the mutant Aβ_{1-40} peptide, which has a valine to alanine substitution (Val18→Ala), has a lower capacity to form amyloid fibrils (*5*), and a greater ability to bind AChE (*11*). Panel C shows that a similar elution pattern was observed when the mutant Aβ peptide was incubated alone (left, retention time ca. 17 min) or with increasing concentrations of the *Torpedo* $H_{274-308}$ peptide. As expected, the mutant Aβ peptide bound more of the *Torpedo* peptide.

The Torpedo AChE Peptide Interacts Directly with Soluble Aβ. The question of whether the *Torpedo* $H_{274-308}$ peptide was incorporated into preexisting amyloid fibrils, or could bind earlier to the Aβ peptide itself (nucleation phase of the Aβ aggregation process), was addressed directly. Since this peptide contains a Trp residue at position 6 (Trp279 in *Torpedo* AChE, Figure 1), we decided to follow its interaction with Aβ by monitoring intrinsic fluorescence. We recorded spectra as early as 15 min after mixing Aβ and $H_{274-308}$, at 25 °C and without stirring, conditions under which no visible aggregates were yet detectable (Figure 3). Figure 6 shows a dose-dependent increase in the intrinsic fluorescence of $H_{274-308}$ (9 μM in the assay) with increasing concentration of Aβ. The increase in fluorescence intensity was accompanied by a blue shift in the emission maximum. Whereas the emission maximum for the *Torpedo* peptide alone is at 355 nm, in the presence of increasing concentrations of Aβ it shifts gradually to 338 nm. This change

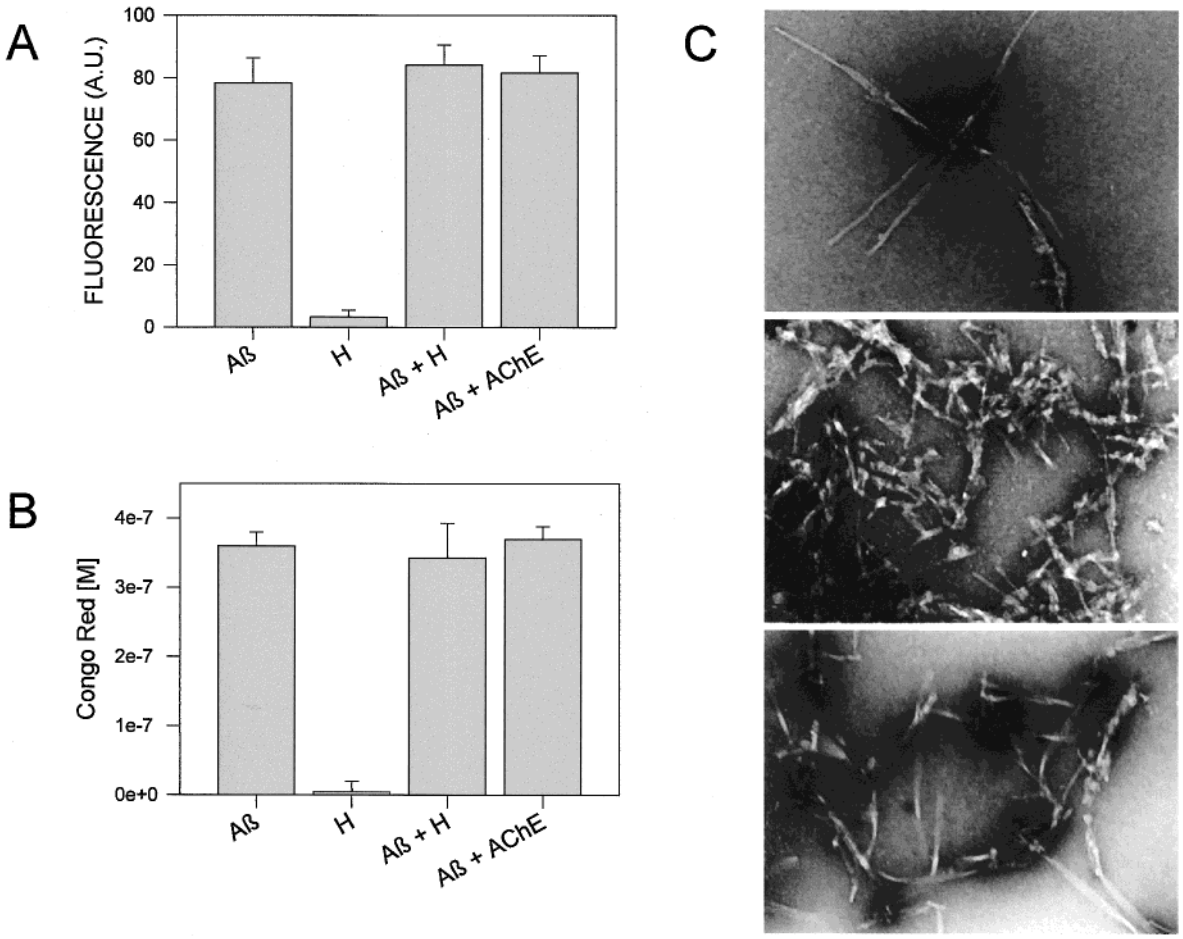

FIGURE 4: Aβ fibrils formed in the presence of the *Torpedo* $H_{274-308}$ peptide are amyloid-positive. Aliquots taken at the end of the aggregation procedure were assayed for amyloid by the Th-T fluorescence method (A), or by use of Congo Red (B). H denotes the hydrophobic peptide. (C) Representative electron micrographs of negatively-stained preparations of Aβ fibrils assembled in the presence of either *Torpedo* AChE or $H_{274-308}$. Top: Aβ fibrils assembled alone. Center: Aβ fibrils assembled in the presence of *Torpedo* AChE. Bottom: Aβ fibrils assembled in the presence of $H_{274-308}$. Original magnification 55000×.

suggests movement of the indole ring of Trp279 from a solvent-exposed to a more hydrophobic environment. Finally, a parallel increase in emission at ca. 310 nm is observed, which may also be ascribed to exposure of the Aβ residue Tyr10 to a more hydrophobic environment.

If we assume that the interaction between Aβ and the *Torpedo* peptide can be represented by the scheme:

$$A\beta + H \rightleftarrows A\beta H$$

where Aβ, H, and AβH are Aβ, the *Torpedo* $H_{274-308}$ peptide, and the stoichiometric complex, respectively, and we further assume that [Aβ] > [H], the following equation can be derived:

$$1/(F - F_0) = 1/K_a F_B[H] + [A\beta]/F_B[H]$$

where F is the experimentally measured fluorescence, F_0 is the fluorescence of the *Torpedo* peptide in the absence of Aβ, F_B is the fluorescence at saturation of Aβ, and K_a is the association constant (*30*). Figure 7A shows the plot obtained using this equation, from which a value of $K_d = 1/K_a = 1.84 \times 10^{-4}$ M was obtained ($K_d = 1.83 \times 10^{-4}$ M, data corresponding to the blue shift; Figure 7D). Similar experiments performed in the presence of 100 mM NaCl showed very similar emission spectra (not shown) and a value of $K_d = 1.76 \times 10^{-4}$ M (Figure 7B). Thus, the data are indicative of a primarily hydrophobic interaction between the two peptides. Finally, titration of $H_{274-308}$ with the mutant Aβ-(Val18→Ala) peptide showed a $K_d = 1.65 \times 10^{-4}$ M (Figure 7C), which was also independent of salt concentration (not shown). Similar binding constants were obtained when interaction of the intact bovine brain AChE molecule with wild-type Aβ was compared with its interaction with the mutant peptide (Alarcón, De Ferrari, and Inestrosa, unpublished results).

DISCUSSION

In addition to the proposed noncholinergic activity of AChE in Aβ deposition in AD brains, there is increasing evidence suggesting noncholinergic roles for the enzyme in cell-adhesion and cell-differentiation processes (*31*−*33*). Moreover, toxic effects, which depend on the concentration of AChE, have been found on neuronal and glial-like cells (*34*). With respect to the interaction of AChE with Aβ, it is worth noting that certain enzymatic characteristics of AChE associated with plaques and tangles (i.e., pH optimum and inhibitor sensitivity) are different from the activity associated with axons and cell bodies (*10*, *35*). We have observed similar abnormal properties for AChE bound to amyloid fibrils in vitro (*36*). This suggests that interaction with Aβ induces slight structural changes in the AChE molecule.

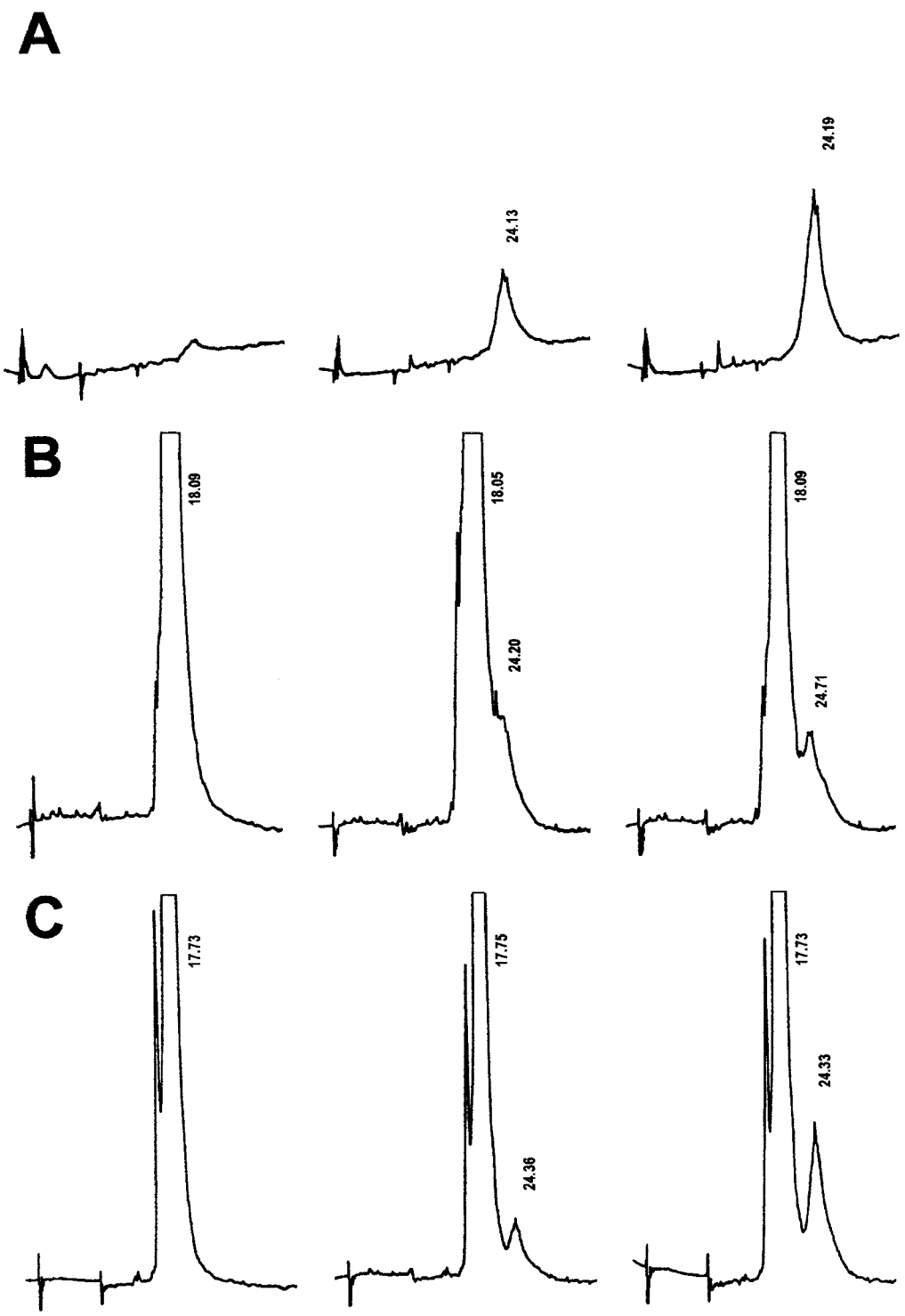

FIGURE 5: *Torpedo* $H_{274-308}$ peptide is incorporated into growing Aβ fibrils in a concentration-dependent manner. Aliquots taken at the end of the aggregation procedure were analyzed by reverse-phase HPLC. (A) *Torpedo* peptide concentration curve (0.1, 0.5, 1 μg). (B) Aβ fibrils grown alone (left) or in the presence of increasing concentrations of the *Torpedo* peptide (molar ratios of Aβ:$H_{274-308}$ = 100:1 and 50:1, respectively). (C) Same as (B) but mutant Aβ(Val18→Ala) fibrils grown alone (left) or in the presence of the *Torpedo* peptide were examined.

In this study, we found that *Torpedo* AChE has four putative docking sites for the modeled Aβ peptides (Figure 2). The experimental data presented demonstrate that the synthetic polypeptide derived from *Site I*, corresponding to the *Torpedo* $H_{274-308}$ sequence, is alone capable of enhancing the rate of amyloid fibril assembly, just as we showed previously for intact AChE (*11*). We have also shown that the *Torpedo* peptide interacts with Aβ already at the nucleation phase of amyloid formation, and is incorporated into the growing fibrils during Aβ aggregation (Figures 3B, 6, and 7). The effect of the peptide appears to be specific, since the mouse $\Omega_{252-275}$ derived peptides do not have a similar effect on the process (Figure 3B). In this latter case, we chose to work with a peptide corresponding to the mouse AChE sequence, rather than the homologous *Torpedo* sequence, since the former sequence, like those

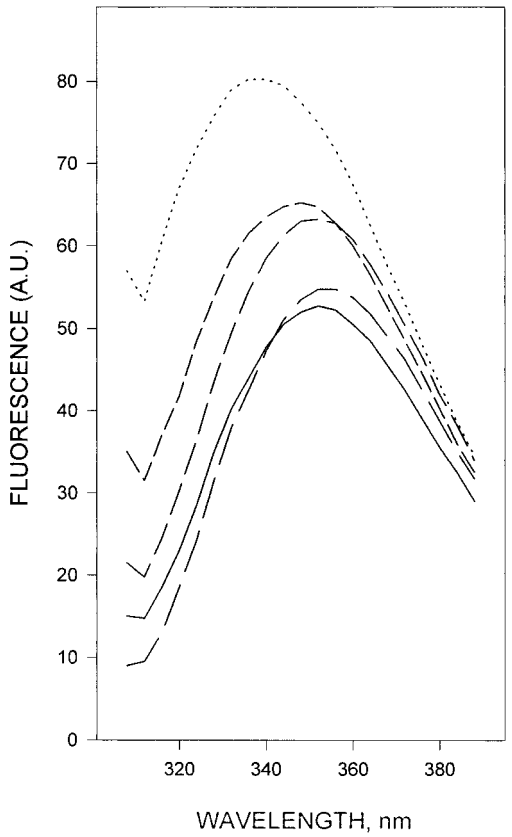

FIGURE 6: Interaction of Aβ with *Torpedo* $H_{274-308}$ peptide changes the intrinsic fluorescence properties of its Trp residue. Representative emission spectra of $H_{274-308}$ alone (9 μM, —) or in the presence of increasing concentrations of Aβ (17 μM, —ThinSpace—; 42.5 μM, – –EnDashEnDash; 85 μM, ---; 170 μM, ···). Emission spectra were recorded between 300 and 400 nm, with excitation at 295 nm, and slits set at 5 nm bandwidth.

in all mammalian AChEs, is four residues longer (see Figure 1). This becomes relevant when *Torpedo* AChE, which lacks these residues, is able to promote amyloid formation in a fashion similar to mammalian AChEs (Figure 3A).

A possible role for the PAS of AChE in amyloid formation was earlier proposed (*11*, *14*), and recent pharmacological experiments suggest that both adhesive and neurotrophic functions of AChE are associated with the PAS (*33*, *37*). The PAS appears to be located close to the lip of the active-site gorge and contains a hydrophobic environment (*38*, *39*). Quantitative analyses of electrostatic surface potentials in the area surrounding the entrance to the gorge have been correlated with an AChE-like motif found in a set of neural cell-adhesion proteins displaying sequence homology with AChE (*40*). The experimental data thus show that *Torpedo* AChE interacts with Aβ through the liposome-interacting domain as a part of docking *Site I* (Figure 8, top). This polypeptide segment, which extends from Glu268 to Lys315, and contains one of the key residues of the PAS (Trp279), "penetrates" the molecule, emerging on the opposite side of the entrance to the gorge, thus creating at least two micromotifs (Figure 8, bottom). The initial sequence that interacts with Aβ in our docking paradigm is Val281–Ser286, which contains residues that are in proximity to the PAS residues, Tyr70 and Trp279. Docking also suggests specific contacts between Pro283 and Gly25, Phe284 and Val24, and Arg289 and Ile32 of *Torpedo* AChE and Aβ, respectively (Figure 9, top). On the opposite side of the gorge, at the C-terminus of the hydrophobic peptide, residues Ser307 and Asn310 of TcAChE make contact with Aβ residues Tyr10 and His6, respectively (Figure 9, bottom). Since none of the modeled Aβ peptides appears to occlude the PAS, it is possible that once the AChE–Aβ complex has been formed, it might modulate the catalytic properties of AChE, as observed in AD brains (*10*), and in the complex of AChE–Aβ in vitro (*36*).

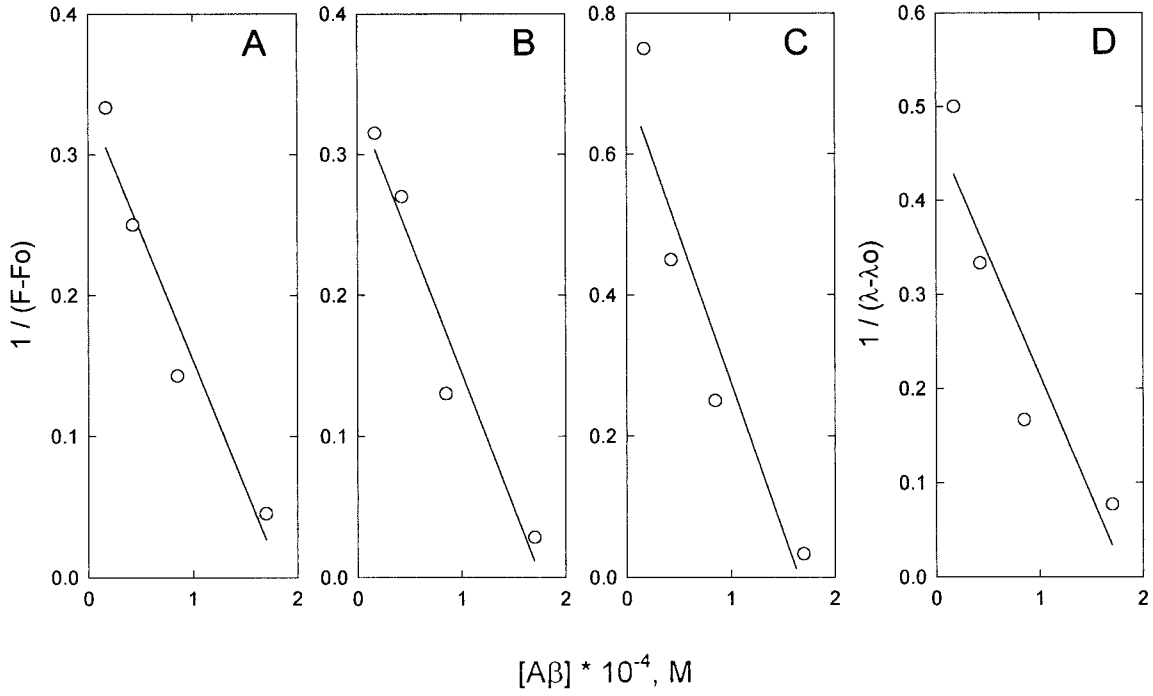

FIGURE 7: Titration of *Torpedo* $H_{274-308}$ peptide with Aβ. Titration of the $H_{274-308}$ peptide with Aβ in the absence (A, D) or presence (B) of 0.1 M NaCl. (C) The (Val18→Ala) Aβ mutant was used. In panels A–C, the plots employ the data for increase in fluorescence intensity; and in panel D, those for the blue shift in the wavelength of the emission.

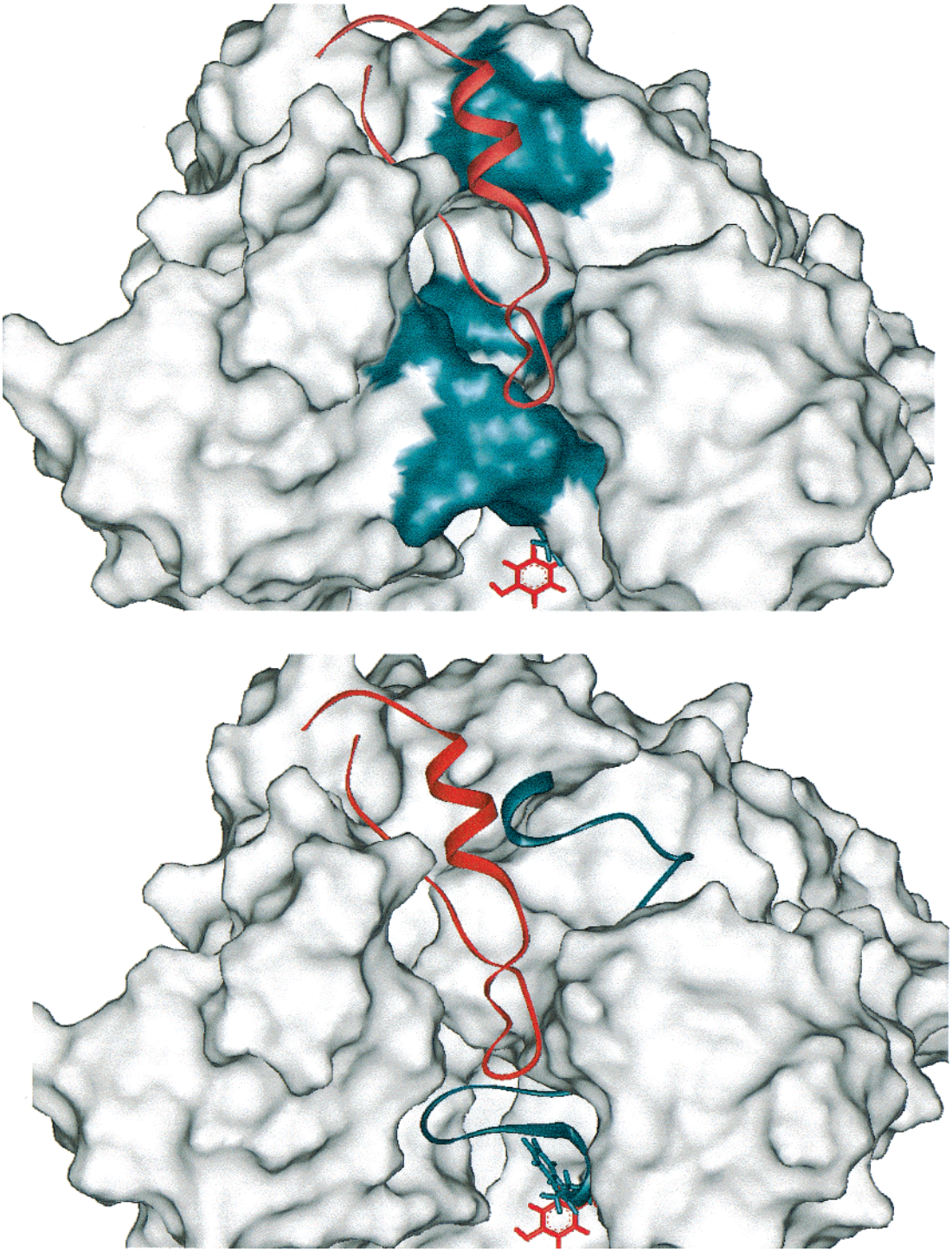

FIGURE 8: Structural disposition of Aβ *Site I* on *Torpedo* AChE. Top: Complementarity of the surface of *Torpedo* AChE (dark green) and Aβ (solid ribbon, dark red) in their complex. PAS residues Tyr70 (red) and Trp279 (dark green) are presented as ball-and-stick models. Bottom: Complementarity of *Torpedo* liposome-interacting domain (dark green) and Aβ (solid ribbon, dark red). Note that the *Torpedo* peptide penetrates close to the entrance of the active-site gorge, emerging at the other site of the gorge, to create two "microdomains". Both "microdomains" may participate in the interaction with Aβ.

The fundamental mechanism of amyloid formation and deposition is under active physicochemical investigation by many groups (*41*). It is clear that amyloid formation can occur for a variety of proteins but, due to the prevalence and severity of Alzheimer's disease, much of this research has centered around the transitional process for the Aβ peptide. Schematically, this transition can be broken up into two steps, viz., a reversible random coil to β-structure transition, followed by irreversible fibril formation (*42*). Several groups have shown that a variety of surfaces can promote amyloid β-sheet formation, including the phospholipid bilayer membrane (*43*), both hydrophilic mica and hydrophobic graphite (*44*), and the air−water interface (*45*). Although these studies do not provide conclusive evidence as to which of the two steps is accelerated at the interface, reduction of the energy barrier for the coil to β-structure transition may play a role (*46*). Our observation that the peptide, like the intact enzyme, can accelerate amyloid formation could be due either to reduction of this energy barrier (*47*) or to its serving as a nucleation template for

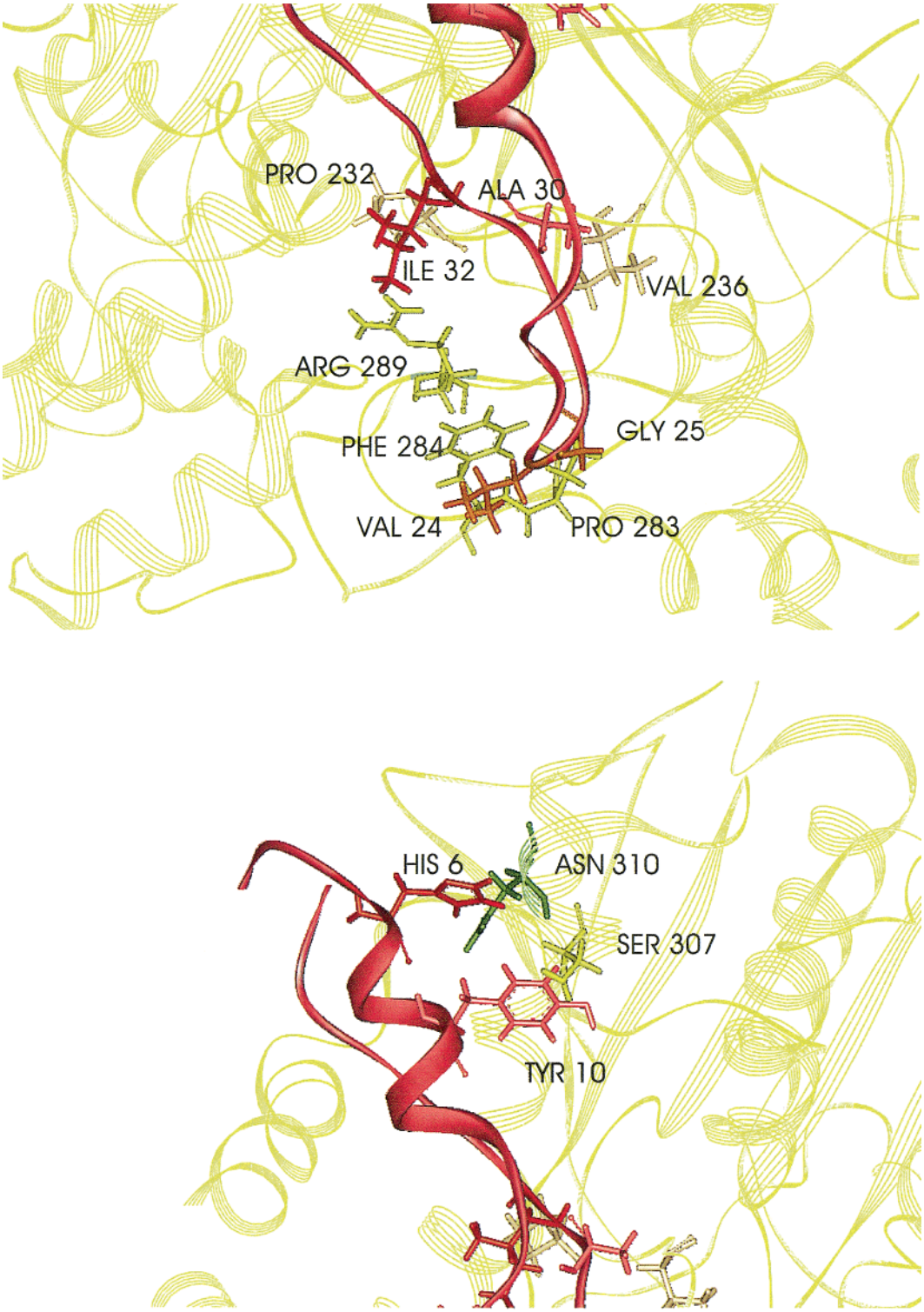

FIGURE 9: Contact sites of Aβ on *Torpedo* AChE. Top: Microdomain close to the gorge of the active site (in the vicinity of the PAS). Bottom: Microdomain at the opposite site of the AChE gorge. Aβ: solid ribbon in dark red color. AChE: line ribbon in dark green color. Interacting residues are depicted as ball-and-stick models.

fibril formation (*48*). Our spectroscopic evidence, directly demonstrating reversible complexation of both the intact enzyme and the synthetic peptide with the Aβ peptide, offers direct support for a role in the first stage, but does not exclude involvement in the nucleation process.

The molecular basis for the interaction of AChE with Aβ is not understood. Here, as a first attempt to identify the AChE−Aβ interaction motif, and considering the yield of our docking paradigm, we chose to work with AChE-derived peptides that had been previously proposed to possess biological activity (*15*, *26*). Although further experiments are needed in order to establish whether other AChE docking sites may also participate in the process of Aβ fibril formation, our data demonstrate that the $H_{274-308}$ peptide derived from docking *Site I* can mimic the noncholinergic activity of AChE on amyloid formation. In this context, it may be noted that Shin et al. (*30*, *49*) have reported that lipid bilayers and micelles can promote a fast structural

transition of native AChE to a partially unfolded molten-globule-like conformation (*50*). Such a structural transition, presumably achieved through the interaction of the whole hydrophobic polypeptide with the membrane, which includes the exposure of both Aβ docking micromotifs identified in this work, has been proposed as an alternative mechanism for insertion of proteins into lipid bilayers (*49*). In a hypothetical scenario, the above observations suggest that similar events may take place in the interaction between these two molecules; viz., Aβ, behaving similarly to a membrane environment, interacts with and partially exposes the hydrophobic segment of AChE, driving the enzyme to a structural intermediate in which the environment of the PAS residues (in particular Trp279) is altered, thus affecting the catalytic characteristics of AChE.

ACKNOWLEDGMENT

We especially thank Drs. Joel L. Sussman and Michal Harel from the Structural Biology Department of the Weizmann Institute of Science for helpful discussions. We also thank Dr. I. Vakser for providing us with the GRAMM program for our docking calculations. I.S. received support from the Israel Ministries of Absorption and Science.

REFERENCES

1. Koo, E. H., Lansbury, P. T., Jr., and Kelly, J. W. (1999) *Proc. Natl. Acad. Sci. U.S.A. 96*, 9989−9990.
2. Kelly, J. W. (1996) *Curr. Opin. Struct. Biol. 6*, 11−17.
3. Selkoe, D. J. (2000) *JAMA, J. Am. Med. Assoc. 283*, 1615−1617.
4. Wilson, C. A., Doms, R. W., and Lee, V. M. (1999) *J. Neuropathol. Exp. Neurol. 58*, 787−794.
5. Soto, C., Castaño, E. M., Frangione, B., and Inestrosa, N. C. (1995) *J. Biol. Chem. 270*, 3063−3067.
6. Harper, J. D., and Lansbury, P. T., Jr. (1997) *Annu. Rev. Biochem. 66*, 385−407.
7. Inestrosa, N. C., and Perelman, A. (1989) *Trends Pharmacol. Sci. 10*, 325−329.
8. Taylor, P. (1991) *J. Biol. Chem. 266*, 4025−4028.
9. Massoulié, J., Pezzementi, L., Bon, S., Krejci, E., and Vallette, F. M. (1993) *Prog. Neurobiol. 41*, 31−91.
10. Geula, C., and Mesulam, M. (1989) *Brain Res. 498*, 185−189.
11. Inestrosa, N. C., Alvarez, A., Pérez, C. A., Moreno, R. D., Vicente, M., Linker, C., Casanueva, O. I., Soto, C., and Garrido, J. (1996) *Neuron 16*, 881−891.
12. Alvarez, A., Opazo, C., Alarcón, R., Garrido, J., and Inestrosa, N. C. (1997) *J. Mol. Biol. 272*, 348−361.
13. Taylor, P., and Lappi, S. (1975) *Biochemistry 14*, 1989−1997.
14. Reyes, A. E., Perez, D., Alvarez, A., Garrido, J., Gentry, M. K., Doctor, B. P., and Inestrosa, N. C. (1997) *Biochem. Biophys. Res. Commun. 232*, 652−655.
15. Bourne, Y., Taylor, P., Bougis, P. E., and Marchot, P. (1999) *J. Biol. Chem. 274*, 2963−2970.
16. Contreras, C. F., Canales, M. A., Alvarez, A., De Ferrari, G. V., and Inestrosa, N. C. (1999) *Protein Eng. 12*, 959−966.
17. Pearlman, D. A., Case, D. A., Caldwell, J. W., Ross, W. S., Cheatham, T. E., III, Fergusson, D. M., Seibel, G. L., Singh, Ch., Weiner, P. K., and Kollman, P. A. (1995) *AMBER 4.1*, University of California, San Francisco.
18. Vakser, I. A. (1995) *Protein Eng. 8*, 371−377.
19. Dixon, J. S. (1997) *Proteins (Suppl. 1)*, 198−204.
20. Inestrosa, N. C., Roberts, W. L., Marshall, T. L., and Rosenberry, T. L. (1987) *J. Biol. Chem. 262*, 4441−4444.
21. Sussman, J. L., Harel, M., Frolow, F., Varon, L., Toker, L., Futerman, A. H., and Silman, I. (1988) *J. Mol. Biol. 203*, 821−823.
22. Lee, S. L., Camp, S. J., and Taylor, P. (1982) *J. Biol. Chem. 257*, 12302−12309.
23. Evans, K. C., Berger, E. P., Cho, C.-G., Weisgraber, K. L., and Lansbury, P. T., Jr. (1995) *Proc. Natl. Acad. Sci. U.S.A. 92*, 763−767.
24. LeVine, H. (1993) *Protein Sci. 2*, 404−410.
25. Klunk, W. E., Pettegrew, J. W., and Abraham, D. J. (1989) *J. Histochem. Cytochem. 37*, 1293−1297.
26. Campos, E., Alvarez, A., and Inestrosa, N. C. (1998) *Neurochem. Res. 23*, 135−140.
27. Shin, I., Silman, I., and Weiner, L. (1996) *Protein Sci. 5*, 42−51.
28. Choo-Smith, L.-P., Garzon-Rodriguez, W., Glabe, C. G., and Surewicz, W. K. (1997) *J. Biol. Chem. 272*, 22987−22990.
29. McLaurin, J. A., Franklin, T., Fraser, P. E., and Chakrabartty, A. (1998) *J. Biol. Chem. 273*, 4506−4515.
30. Shin, I., Silman, I., Bon, C., and Weiner, L. (1998) *Biochemistry 37*, 4310−4316.
31. Koenigsberger, C., Chiappa, S., and Brimijoin, S. (1997) *J. Neurochem. 69*, 1389−1397.
32. Genever, P. G., Birch, M. A., Brown, E., and Skerry, T. M. (1999) *Bone 24*, 297−303.
33. Muñoz, F. J., Aldunate, R., and Inestrosa, N. C. (1999) *NeuroReport 10*, 3621−3625.
34. Calderón, F. H., von Bernhardi, R., De Ferrari, G. V., Luza, S., Aldunate, R., and Inestrosa, N. C. (1998) *Mol. Psychiatry 3*, 247−255.
35. Wright, C. I., Geula, C., and Mesulam, M. M. (1993) *Proc. Natl. Acad. Sci. U.S.A. 90*, 683−686.
36. Alvarez, A., Alarcón, R., Opazo, C., Campos, E., Muñoz, F. J., Calderón, F. H., Dajas, F., Gentry, M. K., Doctor, B. P., De Mello, F. G., and Inestrosa, N. C. (1998). *J. Neurosci. 18*, 3213−3223.
37. Johnson, G., and Moore, S. W. (1999) *Biochem. Biophys. Res. Commun. 258*, 758−762.
38. Sussman, J. L., Harel, M., Frolow, M., Oefner, C., Goldman, A., Toker, L., and Silman, I. (1991) *Science 253*, 872−879.
39. Sussman, J. L., and Silman, I. (1992) *Curr. Opin. Struct. Biol. 2*, 721−729.
40. Botti, S. A., Felder, C., Sussman, J. L., and Silman, I. (1998) *Protein Eng. 11*, 415−420.
41. Wetzel, R. (1999) *Methods Enzymol. 309*, 224−228.
42. Esler, W. P., Stimson, E. R., Mantyth, P. W., and Maggio, J. E. (1999) *Methods Enzymol. 309*, 350−374.
43. Terzi, E., Hölzemann, G., and Seelig, J. (1997) *Biochemistry 36*, 14845−14852.
44. Kowalewski, T., and Holtzman, D. M. (1999) *Proc. Natl. Acad. Sci. U.S.A. 96*, 3688−3693.
45. Schladitz, C., Vieira, E. P., Hermel, H., and Möhwald, H. (1999) *Biophys. J. 77*, 3305−3310.
46. Zhang, S., and Rich, A. (1997) *Proc. Natl. Acad. Sci. U.S.A. 94*, 23−28.
47. Cohen, F. E., Pan, K. M., Huang, Z., Baldwin, M., Fletterick, R. J., and Prusiner, S. B. (1994) *Science 254*, 530−531.
48. Lansbury, P. T., and Caughey, B. (1995) *Chem. Biol. 2*, 1−5.
49. Shin, I., Kreimer, D., Silman, I., and Weiner, L. (1997) *Proc. Natl. Acad. Sci. U.S.A. 94*, 2848−2852.
50. Fink, A. L. (1995) *Annu. Rev. Biophys. Biomol. Struct. 24*, 495−522.

BI0101392